# Drifting Pulses of Traveling-Wave Convection

Paul Kolodner
*AT&T Bell Laboratories, Murray Hill, New Jersey 07974-2070*
(Received 7 December 1990)

I describe experiments on "pulses" of convective traveling waves in an ethanol/water mixture contained in an extremely uniform annular cell. In contrast to previous observations, I find that pulses drift continuously, with no long-term change in velocity. The drift velocity vanishes at onset, increases with the distance above onset, and agrees with the results of numerical integrations of the Navier-Stokes equations.

PACS numbers: 47.25.Qv, 47.20.Ky

Several recent experiments have explored the properties of confined states of traveling-wave (TW) convection in binary fluids in annular containers.[1,2] In these experiments, which used ethanol/water mixtures with separation ratios in the range $-0.09 \lesssim \psi \lesssim -0.07$, the first dynamical state seen above the onset of convection consisted of narrow patches of traveling waves with a fixed spatial profile. This profile was shown[1] to match the functional form of a "pulse" solution of a subcritical Ginzburg-Landau equation in an unbounded geometry,[3] suggesting that the experimental localized states are indeed pulses in the sense of Ref. 3. However, except for transients, the experimental pulses were observed to be *stationary*. This presents a serious conflict with expectations based on the simplest subcritical Ginzburg-Landau equation, because localized TW states should propagate uniformly in space with the group velocity of linear waves in this model.[3] The addition of nonlinear gradient terms to this equation has been shown to cause pulse solutions to propagate more slowly than this.[4] However, the fact that experimental pulses do not drift at all suggests that some other physics beyond the scope of Ginzburg-Landau models—such as an interaction between the convective flow fields and the cell walls—is playing a role in this system. Thus, the stationarity of experimental pulses seems to constitute a major obstacle to their understanding on the basis of model equations.

This paper reports observations of traveling-wave pulses in an extremely uniform annular cell. In contrast with previous observations, I find that pulses drift continuously, with no long-term change in velocity. The drift velocity $v_{dr}$ vanishes at onset and increases with the distance $\varepsilon$ above onset. Because of this sensitive dependence $\varepsilon$, $v_{dr}$ follows local nonuniformities in the cell, which can be measured independently. This sensitivity to nonuniformities suggests an explanation of why pulses were previously observed to slow down and stop. The measured value of $v_{dr}$ agrees reasonably well with recent numerical calculations based on the Navier-Stokes equations.[5] These results resolve an apparent disagreement between numerical theory and experiment, and they present a fresh theoretical challenge: to explain the dependence $v_{dr}(\varepsilon)$. More importantly, they suggest that a theoretical model based on a Ginzburg-Landau equation may be a valid approach to understanding this system after all.

The apparatus has evolved slightly from a previously described version.[2] The cell is an annular channel of height $d = 0.313$ cm, radial width $1.66d$, and mean circumference $76.0d$ which is formed by a plastic disk and ring that are clamped between a heated, mirror-polished silicon bottom plate and a water-cooled sapphire top plate. It has been crucial to make this cell as geometrically and thermally uniform as possible, and an assessment of the uniformity is given below. Pulses were studied using a 1.45-wt% ethanol/water solution at a mean temperature of 26.9 °C, for which the separation ratio $\psi = -0.072$, the Prandtl number $P = 6.69$, and the Lewis number $L = 0.009$.[6] The temperature difference applied across the fluid is typically 3.5 K and is regulated with a stability of $\pm 0.2$ mK. The onset temperature difference exhibits no measurable drift with time, indicating that there are no leaks in the cell which might cause localized concentration changes.[2] The flow is visualized by shadowgraphy.[2,7] The shadowgraph image is directed onto an annular array of 720 photodiodes, whose output is sampled at regular time intervals by a small computer. The data processing employed is described below. The convective patterns are always observed to be one dimensional, consisting of superpositions of waves which travel azimuthally around the cell in opposite directions ("left" and "right").

The linear TW instability which triggers the onset of convection in this system is an excellent tool for assessing its uniformity. The techniques used for controlling the linear TW have been described previously.[7,8] Using a fluid with $\psi = -0.021$, I increased the temperature difference across the cell until oscillations due to the instability were observed in the shadowgraph. The amplitude profiles $A_{L,R}(x)$ of the corresponding left and right TW ($x$ denotes the spatial position in the cell) were computed in real time by the computer, using complex demodulation techniques.[7] By adjusting the temperature difference across the cell so that the sum of the spatially

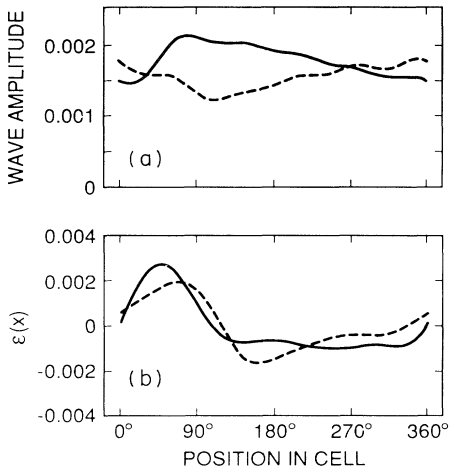


FIG. 1. (a) Left (dashed line) and right (solid line) wave amplitude profiles $A_{L,R}(x)$ vs spatial position $x$, for a steady state of linear waves exactly at onset, using a fluid with $\psi=-0.021$. Both profiles exhibit spatial growth in the region 0°–90° and spatial decay in the region 90°–360°. (b) Local stress parameter $\varepsilon(x)$ derived from the amplitude profiles above using Eq. (1). The two curves agree reasonably well and exhibit nonuniformities of better than about $\pm 0.2\%$.

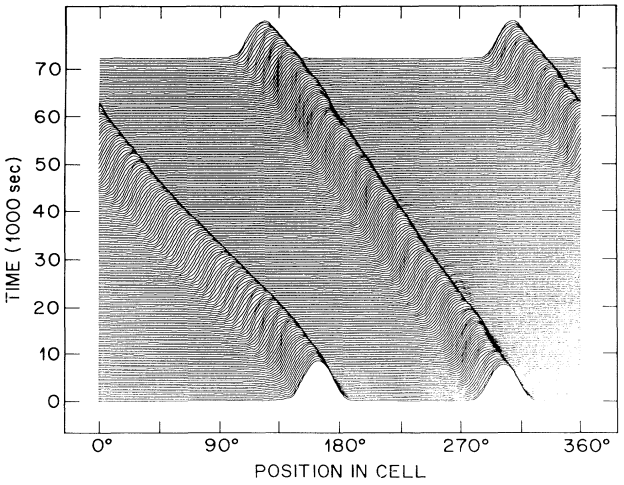


FIG. 2. Hidden-line plot of the amplitude profiles of a state consisting of two pulses of left-going TW, at $\bar{\varepsilon}=0.0090$. Both pulses drift continuously to the left.

averaged amplitude profiles exhibits zero temporal growth rate, the system is servoed at the linear onset, and a steady pattern of linear TW is allowed to evolve. The amplitude profiles of this state are shown in Fig. 1(a). These profiles are far more uniform than have been obtained previously.[8] The wave numbers of the left and right TW components are also spatially uniform and equal to within about $\pm 0.5\%$.

The linear TWs are quantitatively described by the linear part of a complex Ginzburg-Landau equation[9]

$$\tau_0\left(\frac{\partial A_{L,R}}{\partial t}\pm s\frac{\partial A_{L,R}}{\partial x}\right)=\varepsilon(x)(1+ic_0)A_{L,R}+\xi_0^2(1+ic_1)\frac{\partial^2 A_{L,R}}{\partial x^2}. \quad (1)$$

In order to model nonuniformities in the cell, I allow the stress parameter $\varepsilon$ to have a weak spatial dependence. [The experimentally measured fraction by which the temperature difference $\Delta T$ applied across the cell exceeds the onset of convection $\Delta T_c$, which I denote $\bar{\varepsilon}\equiv(\Delta T-\Delta T_c)/\Delta T_c$, corresponds to the spatial average of $\varepsilon(x)$.] All the other parameters in Eq. (1) have been defined in Ref. 9 and are accurately known. Thus, the measurements of $A_{L,R}(x)$ can be substituted into Eq. (1) to yield two estimates for $\varepsilon(x)$. These are shown in Fig. 1(b). $\varepsilon(x)$ is uniform to better than $\pm 0.2\%$. The key to this extreme uniformity is the use of compliant O rings to seal the cell. By clamping the cell together under an interferometer against the resistance of the O rings, I am able to stably adjust the cell height with a spatial uniformity of better than $\pm 0.3$ $\mu$m. Without compliant O rings, the cell flatness can be 20 times worse.

After this assessment of uniformity was made, the cell was filled with the fluid with $\psi=-0.072$. As in previous experiments at similar $\psi$,[1,2] the first convective state observed just above onset takes the form of one or more TW pulses. Their spatial amplitude profiles are computed at each time step using spatial demodulation of the shadowgraph image at the measured mean wave number.[2] A hidden-line plot of the evolution of a two-pulse, left-going state is shown in Fig. 2. As in previous experiments, these pulses have a FWHM of approximately 5 times the cell height. However, in contrast to previous observations, they drift continuously in the direction of the phase velocity of the underlying TW. I have created one-, two-, and three-pulse states and pulses which drift in either direction. Pulses have been observed to travel continuously for days at constant $\bar{\varepsilon}$, circling the cell several times with no apparent long-term change in velocity. Because of this drift, counterpropagating pulses are always removed from the system by annihilation events of the type described in Ref. 2.

For quantitative characterization of pulse drift, I calculate the spatial position of each pulse by computing the first moment of its amplitude profile. Differentiating in time gives the drift velocity $v_{dr}$, which is scaled by $\kappa/d$, where $\kappa$ is the thermal diffusivity of the fluid, and $d$ is the cell height. Figure 3 shows the spatial dependence of the $v_{dr}(x,\bar{\varepsilon})$ for several different values of $\bar{\varepsilon}$ ($v_{dr}<0$ for left-going pulses; from here on, I will only consider the absolute value of $v_{dr}$). The magnitude of the average drift velocity increases with $\bar{\varepsilon}$. Aside from this, the spatial structure of $v_{dr}(x,\bar{\varepsilon})$ is reproducible from run to run, and from pulse to pulse in a given run. As shown below, this is just because $v_{dr}(x,\bar{\varepsilon})$ is sensitive to the local value

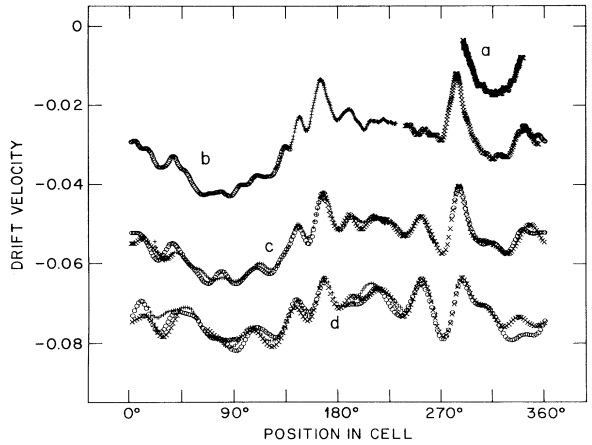


FIG. 3. Absolute value of the drift velocity $v_{dr}$ vs spatial position for several different left-going pulses. (a) Single-pulse state, $\bar{\varepsilon}=0.0027$. (b) Triple-pulse state, $\bar{\varepsilon}=0.0065$. The three pulses are represented by +, ○, and ×. (c) Triple-pulse state, $\bar{\varepsilon}=0.012$. (d) Triple-pulse state, $\bar{\varepsilon}=0.017$. The absolute value of the average drift velocity increases with increasing $\bar{\varepsilon}$. The spatial structure of $v_{dr}(x)$ is reproducible from run to run as well as from pulse to pulse in a single run.

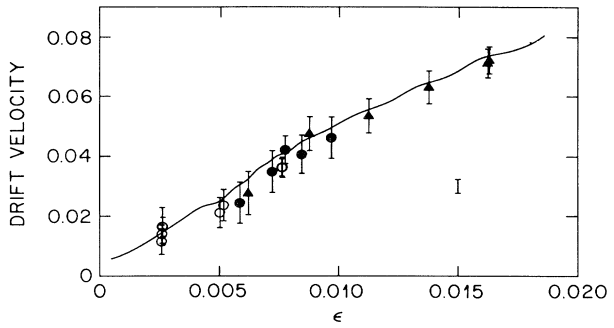


FIG. 4. Drift velocity $v_{dr}$ vs stress parameter $\varepsilon$. Each discrete symbol represents the spatially averaged value $\bar{v}_{dr}$ in a run like those in Fig. 3, plotted at the value of $\bar{\varepsilon}$ for that run. The error bars represent twice the standard deviation of the spatial variation of $v_{dr}$ for each point. Open circles: single-pulse states. Solid circles: double-pulse states. Triangles: triple-pulse states. The smooth curve is the binned and averaged drift velocity which results from the removal of the spatial variation of $\varepsilon(x)$, and the size of the isolated error bar is twice the average standard deviation for the individual bins.

of $\varepsilon(x)$.

From nineteen runs at various values of $\bar{\varepsilon}$, I extract 6445 separate measurements of $v_{dr}(x,\bar{\varepsilon})$. These data are used as inputs to an iterative procedure for deducing both the intrinsic dependence of $v_{dr}$ on $\varepsilon$ and the spatial dependence of $\varepsilon(x)$, which is then compared with that in Fig. 1(b). I start by simply plotting the spatially averaged drift velocity $\bar{v}_{dr}$ for each run versus $\bar{\varepsilon}$. These data are represented by the nineteen discrete symbols in Fig. 4. The error bars are due to the spatial variation of $v_{dr}$. At this level, the principal result of this paper is already evident: $\bar{v}_{dr}$ increases roughly linearly with $\bar{\varepsilon}$. To within the error bars, multiple-pulse states drift at the same velocity as single-pulse states.

$\varepsilon$ is then parametrized as a function of $v_{dr}$ by fitting a line to the nineteen data points in Fig. 4. Then, for each of the 6445 measurements of $v_{dr}(x,\bar{\varepsilon})$, the fitted $\varepsilon(v_{dr})$ is used to calculate the stress-parameter nonuniformity $\delta\varepsilon(x)=\varepsilon(v_{dr}(x,\bar{\varepsilon}))-\bar{\varepsilon}$. If the dependence $v_{dr}(\varepsilon)$ is close to linear, then $\delta\varepsilon(x)$ should match the curve in Fig. 1(b). The results for $\delta\varepsilon(x)$ are binned in space and averaged to produce the solid curve in Fig. 5; the error bar is twice the average of the standard deviations in the individual bins. For comparison, the dashed curve is the average of the two estimates for $\varepsilon(x)$ shown in Fig. 1(b), *shifted to the right* by 21°, which corresponds to 4.4 times the cell height, or approximately one pulse width. The demodulation result, which is intrinsically low-pass filtered, exactly matches the low-spatial-frequency component of $\delta\varepsilon(x)$. That two measurements of $\delta\varepsilon(x)$ based on different dynamical states agree so well constitutes strong confirmation of both. The pulse velocity depends on the stress parameter measured $4d$ to $5d$ ahead of its center.

The iterative procedure can be carried further to decrease the error bars in Fig. 4. The data in Fig. 5 allow the calculation of the true local stress parameter $\varepsilon(x,\bar{\varepsilon})=\bar{\varepsilon}+\delta\varepsilon(x)$, and thus the $x$ dependence can be removed from the 6445 measurements of $v_{dr}(x,\bar{\varepsilon})$. The resulting points are binned in $\varepsilon$ and averaged, and the smooth curve in Fig. 4 is a spline fit to the binned points. As shown by the isolated error bar in Fig. 4, the uncertainty in $v_{dr}(\varepsilon)$ has been reduced by about a factor of 2. Higher-quality data taken since the original submission of this paper are very well fitted by a function of the form $v_{dr}(\varepsilon)=-v_0+a(\varepsilon+\varepsilon_0)^{1/2}$. With $v_0=0.051$, $a=0.89$, and $\varepsilon=0.0025$, this function fits the original 6445 data points in Fig. 4 with a rms error of 0.003. These results clarify several recent experimental observations. In Refs. 1 and 2, pulses were always observed to

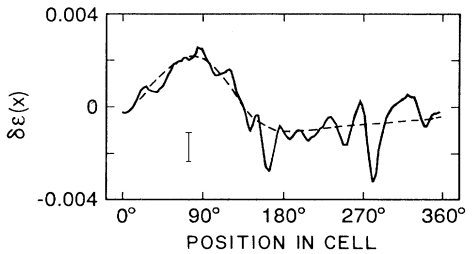


FIG. 5. Solid curve: binned and averaged values of the stress-parameter nonuniformity $\delta\varepsilon(x)$, as deduced from pulse-velocity data. The error bar represents twice the average of the standard deviations in each of the bins. Dashed curve: average of the two curves for $\varepsilon(x)$ shown in Fig. 1(b), shifted to the right by 21° or $4.4d$.

slow down and stop after changes in $\bar{\varepsilon}$. At the small values of $\bar{\varepsilon}$ used in previous work ($\bar{\varepsilon} \leq 0.008$), a nonuniformity only 6 times worse than that in Fig. 5 will guarantee that there is always a region of negative $\varepsilon$ in the cell. Since $v_{dr}$ drops to zero at $\varepsilon = 0$, this means that pulses will drift through the region of positive $\varepsilon$, slow down, and stop.[10] I estimate that this was the case in my own previous experiments. In Ref. 2, my collaborators and I observed that left- and right-going pulses always seemed to come to a stop at the same two separate locations, which faced each other and which were about $20d$ apart. This was independent of the initial location of pulse formation and of the number of pulses. It now seems clear that this was because our previous cell had a single local minimum in $\delta\varepsilon(x)$, about $11d$ wide.

Barten, Lücke, and Kamps[5] have recently computed a localized two-dimensional TW solution of the full Navier-Stokes equations for $\psi = -0.08$ which appears to be identical to the experimentally observed pulses.

The numerical pulse is observed to drift slowly in the direction of the phase velocity of the TW, in agreement with my observations. Because the drift and phase velocities of the pulse, as well as the linear phase velocity, are probably affected by the narrow width of experimental cells, it is difficult to compare the absolute velocities calculated in two dimensions with experimental measurements. For this reason, these authors quote not absolute velocities but ratios: For $\varepsilon = 0.008$, they find $v_{phase}/v_{dr} \sim 15$ and $v_{linear}/v_{dr} \sim 35$. For the same $\bar{\varepsilon}$, I measure 16 and 47, respectively; the first number has an uncertainty of about 20% because of the difficulty in defining the phase velocity. I regard this agreement as good, considering the uncertain effects of cell width. The challenge to theory is now to construct a reduced model of this system which accounts for this slow drift velocity and its dependence on $\varepsilon$.

I thank P. C. Hohenberg and C. M. Surko for useful discussions.

[1]J. J. Niemala, G. Ahlers, and D. S. Cannell, Phys. Rev. Lett. **64**, 1365 (1990); K. E. Anderson and R. P. Behringer, Phys. Lett. A **145**, 323 (1990).

[2]P. Kolodner and J. A. Glazier, Phys. Rev. A **42**, 7504 (1990); J. A. Glazier and P. Kolodner, Phys. Rev. A (to be published).

[3]O. Thual and S. Fauve, J. Phys. (Paris) **49**, 1829 (1988); W. van Saarloos and P. C. Hohenberg, Phys. Rev. Lett. **64**, 749 (1990); (to be published).

[4]H. R. Brand and R. J. Deissler, Phys. Rev. Lett. **63**, 2801 (1989); R. J. Deissler and H. R. Brand, Phys. Lett. A **146**, 252 (1990).

[5]W. Barten, M. Lücke, and M. Kamps (to be published).

[6]P. Kolodner, H. Williams, and C. Moe, J. Chem. Phys. **88**, 6512 (1988).

[7]P. Kolodner and H. Williams, in *Proceedings of the NATO Advanced Research Workshop on Nonlinear Evolution of Spatio-Temporal Structures in Dissipative Continuous Systems*, edited by F. H. Busse and L. Kramer, NATO Advanced Study Institute, Ser. B2, Vol. 225 (Plenum, New York, 1990), p. 73.

[8]P. Kolodner, J. A. Glazier, and H. Williams, Phys. Rev. Lett. **65**, 1579 (1990).

[9]M. C. Cross and K. Kim, Phys. Rev. A **37**, 3909 (1988).

[10]Measurements at $\psi = -0.10$, which I will report on in detail in the future, indicate that $v_{dr} \approx 0$ for $\bar{\varepsilon} < 0$.